PAPER

Bubble growth from clustered hydrogen and helium atoms in tungsten under a fusion environment

To cite this article: Yu-Wei You *et al* 2017 *Nucl. Fusion* **57** 016006

IOP Publishing | International Atomic Energy Agency Nuclear Fusion

Nucl. Fusion **57** (2017) 016006 (10pp) doi:10.1088/0029-5515/57/1/016006

Bubble growth from clustered hydrogen and helium atoms in tungsten under a fusion environment

Yu-Wei You[1], Xiang-Shan Kong[1], Xuebang Wu[1], C.S. Liu[1], J.L. Chen[2] and G.-N. Luo[2]

[1] Key Laboratory of Materials Physics, Institute of Solid State Physics, Chinese Academy of Sciences, PO Box 1129, Hefei 230031, People's Republic of China
[2] Institute of Plasma Physics, Chinese Academy of Sciences, Hefei 230031, People's Republic of China

E-mail: xbwu@issp.ac.cn (Xuebang Wu), and csliu@issp.ac.cn (Changsong Liu)

Received 15 April 2016, revised 30 August 2016
Accepted for publication 12 September 2016
Published 3 October 2016

Abstract

Bubbles seriously degrade the mechanical properties of tungsten and thus threaten the safety of nuclear fusion devices, however, the underlying atomic mechanism of bubble growth from clustered hydrogen and helium atoms is still mysterious. In this work, first-principles calculations are therefore carried out to assess the stability of tungsten atoms around both hydrogen and helium clusters. We find that the closest vacancy-formation energies of interstitial hydrogen and helium clusters are substantially decreased. The first-nearest and second-nearest vacancy-formation energies close to vacancy–hydrogen clusters decrease in a step-like way to ∼0, while those close to vacancy–helium clusters are reduced almost linearly to ∼−5.46 eV when atom number reaches 10. The vacancy-formation energies closest to helium clusters are more significantly reduced than those nearest to hydrogen clusters, whatever the clusters are embedded at interstitial sites or vacancies. The reduction of vacancy-formation energies results in instability and thus emission of tungsten atoms close to interstitial helium and vacancy–helium clusters, which illustrates the experimental results, that the tungsten atoms can be emitted from the vicinity of vacancy–helium clusters. In addition, the emission of unstable tungsten atoms close to hydrogen clusters may become possible once they are disturbed by the environment. The emission of tungsten atoms facilitates the growth and evolution of hydrogen and helium clusters and ultimately the bubble formation. The results also explain the bubble formation even if no displacement damage is produced in tungsten exposed to low-energy hydrogen and helium plasma.

Keywords: nulclear fusion, tungsten, hydrogen and helium bubble

(Some figures may appear in colour only in the online journal)

1. Introduction

Controlled thermonuclear fusion energy, a sort of clean and infinite energy source, is believed to be able to thoroughly solve the energy crisis mankind faces. The international thermonuclear experimental reactor (ITER) is an international project for developing a fusion device of self-sustaining combustion and demonstrating the scientific and technological feasibility of fusion energy for peaceful purposes [1]. In the fusion device, extended burn of deuterium–tritium (D–T) plasma will be conducted. High-energy neutrons (up to 14 MeV), D, T and helium (He) ions which escape from the D–T plasma cause the degradation of the mechanical properties and structural strength of the plasma-facing materials (PFMs). Tungsten (*W*), a high-Z material, has been chosen to be the PFM in ITER [1] due to its excellent properties of high melting point, good thermal conductivity, excellent high-temperature strength and low sputtering rate. However, in the

fusion device, irradiation of high fluxes of D, T and He ions and neutrons can also lead to displacement damage, bubble and fuzz formation [2–5]. It is generally agreed that bubbles are not desirable because such features degrade the mechanical properties of tungsten by presenting areas of high strain fields and easy initiation of failure by embrittlement or stress corrosion cracking. Therefore, it is essential to understand the underlying reasons for bubble formation, which associates with the interactions of H and He with vacancy-type defects in tungsten.

It is widely realized that H and He atoms are energetically favorable to cluster in vacancies [6–9]. The clustering of H and He atoms in vacancies, in turn, influences the vacancy evolution. Fukai *et al* found that H can stabilize and increase the concentration of a vacancy [10–12]. In many experiments, it is found that even if there is no vacancy produced in tungsten exposed to low-energy D ions, there is bubble formation in the material. For example, many experiments showed that D plasmas with energy of tens of eV definitely produce bubbles in tungsten [13–17]. Ogorodnikova *et al* proposed that several D atoms trapped in a monovacancy could cause the displacement of neighboring lattice atoms due to stress-induced atomic diffusion, creating a divacancy and thus initiating bubble growth [18]. Similarly, low-energy He ion irradiation can also result in bubble formation and subsequent degradation of the mechanical properties of tungsten. Experimental results have shown that bubbles are formed in W as long as the incident He ion energy is above 5 eV [19]. By performing molecular dynamics simulations, Henriksson *et al* suggested W atoms can be displaced nearby a He_n cluster towards the surface [20, 21]. In our previous work [22], it was found that the emission of tungsten atoms close to vacancy–helium clusters, $VacHe_n$, is possible once n is beyond 9, which agrees well with the experimental results that the emission of tungsten atoms close to $VacHe_n$ becoming Vac_2He_n happens when n is about 10 [23]. With the same method we found that the emission of tungsten atoms around $VacH_n$ clusters seems difficult without being influenced by other conditions. Our previous work mainly focused on the influence of dissolution energy on the emission of tungsten atoms around hydrogen and helium clusters at interstitial sites and vacancies. However, the vacancy-formation energy, namely tungsten-atom stability, also affects the tungsten atom emission around H and He clusters, and little attention has been paid to the stability of tungsten atoms nearby the two kinds of clusters yet.

In this paper, we perform systematical first-principles calculations to access the stability of tungsten atoms around Vac_mH_n and Vac_mHe_n clusters. The aim is to evaluate the reasons controlling the emission of the tungsten atoms around Vac_mHe_n clusters, and compare the stability of tungsten atoms around Vac_mH_n and Vac_mHe_n clusters. We find that vacancy-formation energies closest to both Vac_mH_n and Vac_mHe_n clusters are significantly reduced. The vacancy-formation energies closest to Vac_mHe_n clusters are fairly more reduced than that nearest to Vac_mH_n clusters. The underlying reasons for the reduction of vacancy-formation energy are analyzed.

2. Computational method

The calculations in this paper are done within density functional theory as implemented in the Vienna *ab initio* simulation package (VASP) with the projector-augmented wave potential method [24, 25]. The generalized gradient approximation and the Perdew–Wang functional are used to describe the electronic exchange and correlation effect [26]. The supercells composed of $4 \times 4 \times 4$ and $5 \times 5 \times 5$ lattice points are used. The free optimizations of atomic position, and supercell shape and size are performed. The plane-wave cutoff and k-point density, obtained using the Monkhorst–Pack method [27], are both checked for convergence for each system to be within 0.001 eV per atom. A plane-wave cutoff of 500 eV and a k-point grid density of $3 \times 3 \times 3$ are employed in all the calculations. The structural optimization is truncated when the forces converge to less than 0.01 eV Å^{-1}. The $4 \times 4 \times 4$ supercell is used in all the calculations unless otherwise specified. The defect-formation energies are computed by the following formula:

$$E_f = E_{tot}^{nW,mX} - nE^W - mE^X, \quad (1)$$

where X indicates H or He, $E_{tot}^{nW,mX}$ is the total energy of the system with n W atoms and m X atoms, E^W is the energy per atom of pure crystal W, and E^X is one half of the energy of a H_2 molecule or the energy of an isolated He atom. The half energy of a H_2 molecule is calculated to be -3.40 eV, which agrees well with the value from Liu *et al* [6]. The binding energies of interstitial X atoms clusters are determined for different configurations, which is expressed by:

$$E_b(X_n) = nE_{tot}(X_{tet}) - E_{tot}(X_n) - (n-1)E_{tot}(p), \quad (2)$$

where $E_{tot}(X_n)$ is the energy of the W system containing X_n clusters, $E_{tot}(X_{tet})$ is the total energy of the W system with an X atom situated at a tetrahedral interstitial site in tungsten, and $E_{tot}(p)$ is the total energy of pure crystal W. In such a scheme, a positive binding energy indicates attractive interaction while a negative value means a repulsive interaction. When the number of X atoms is increased from $n-1$ to n in a vacancy, the binding energy is defined as:

$$E_b(VacX_n) = E_{tot}(VacX_{n-1}) + E_{tot}(X_{tet}) - E_{tot}(VacX_n) - E_{tot}(p), \quad (3)$$

where n is the number of X atoms and $E_{tot}(VacX_n)$ is the total energy of the system with n X atoms in a vacancy, $E_{tot}(X_{tet})$ is the total energy of the W system with a tetrahedral interstitial defect. A negative value of $E_b(VacX_n)$ indicates taking an interstitial X atom and adding it to a vacancy that already contains $(n-1)$ X atoms which is energetically favorable, with $|E_b(VacX_n)|$ being the energy gained in that process. Here, we specially calculate the vacancy-formation energies close to Vac_mX_n clusters using the following equation:

$$E_f(Vac) = E_{tot}(Vac_mX_n) - E^W - E_{tot}(Vac_{m+1}X_n), \quad (4)$$

where $E_{tot}(Vac_mX_n)$ is the total energy of the system containing Vac_mX_n clusters. The binding energy of a vacancy cluster in the presence of X is calculated by:

Table 1. The vacancy-formation energy E_f(Vac) (in eV) of the *W* atom that has multiple neighboring interstitial *X* (*X* = *H* or He) atoms is calculated.

X_n	$E_b(X_n)$	$E_b^{Ref}(X_n)$	E_f (Vac)
H_1	—	—	1.99
H_2	0.00	0.02[a]	0.83
H_3	−0.01	—	−0.27
H_4	−0.06	—	−1.34
H_5	−0.11	—	−2.14
H_6	−0.12	—	−2.98
He_1	—	—	−1.36
He_2	1.07	1.03[b]	−3.41
He_3	2.55	2.39[b]	−5.07
He_4	4.44	3.90[b]	−6.59
He_5	6.50	5.54[b]	−6.87
He_6	8.85	—	−7.25

[a] Liu *et al* [30]
[b] Becquart *et al* [31].
Note: Meanwhile, the binding energy E_b(in eV) of these *X* atoms is also calculated using equation (2).

$$E_b(\mathrm{Vac}_m X_n) = mE_{tot}(\mathrm{Vac}) + nE_{tot}(X_{tet}) - E_{tot}(\mathrm{Vac}_m X_n) - (m+n-1)E_{tot}(p). \quad (5)$$

In order to determine the migration properties of $VacH_n$ and $VacHe_n$ clusters in tungsten between different minima, the nudged elastic band method is employed.

3. Results

3.1. The stability of tungsten atoms close to interstitial hydrogen and helium clusters

We firstly study the stability of H and He atoms at interstitial sites in tungsten. The results suggest that both H and He prefer to occupy a tetrahedral interstitial site (TIS) rather than an octahedral interstitial site (OIS). The energy differences of H and He at an OIS and a TIS are 0.39 eV and 0.21 eV, respectively. These results are in good agreement with the reported data [28, 29]. The H–H binding energy is negative, and the binding energy approaches zero when the distance is larger than 2.0 Å. The binding energy of the interstitial He–He pair is 1.07 eV when the two He atoms are separated by 1.5 Å. This indicates that the formation of interstitial He clusters is energetically favorable. The binding energies of interstitial H and He clusters are then calculated and presented in table 1, where the available references are also summarized. From the table, it is noted that the binding energies of H_2 and He_2 agree well with the reported data [30, 31]. The binding energies of He_3, He_4 and He_5 clusters are generally larger than the values obtained by Becquart *et al* [31]. This may originate from the fact that our calculated close-packed monolayer He interstitial cluster is more stable [22]. From the table, one can also see that the interstitial H cluster presents weak repulsive interaction.

Once the interstitial H and He clusters in perfect tungsten are formed, the presence of clusters will inevitably induce local stress, which may affect the stability of tungsten atoms close to the clusters. Thus, the effects of interstitial H and He clusters on the vacancy formation have been studied. The formation energy of a vacancy in the vicinity of H clusters can be approximated by the equation (4), and the values close to interstitial H_1, H_2, H_3, H_4, H_5 and H_6 clusters are calculated to be 1.99 eV, 0.83 eV, −0.27 eV, −1.34 eV, −2.14 eV and −2.98 eV, respectively. Thus, the vacancy-formation energies are reduced and H clusters are able to affect the stability of tungsten atoms close to the clusters. However, the emission of tungsten atoms from the vicinity of interstitial H clusters is difficult without being disturbed by other conditions according to our work [22]. The presence of interstitial He clusters in tungsten will have even greater influence on the stability of tungsten atoms close to the clusters. The vacancy-formation energy close to a single interstitial He atom is reduced to −1.36 eV. When the He atoms are increased in the interstitial cluster, the nearby vacancy-formation energies are further decreased. A He_6 cluster can decrease the vacancy-formation energy to −7.25 eV. The stability of tungsten atoms close to He clusters are significantly decreased due to the remarkable reduction of vacancy-formation energy, and thus the emission of the tungsten atoms becomes possible. This may be the reason why tungsten atoms can be emitted from the vicinity of interstitial He clusters when the He atom number in the cluster is beyond 5, as found in our previous work [22]. Once the tungsten atoms are emitted, the He atoms in the cluster will move spontaneously to the vacancy produced nearby.

3.2. The stability of tungsten atoms around $VacH_n$ and $VacHe_n$ clusters

H and He can diffuse with barriers as small as 0.2 eV [32] and 0.06 eV [31, 32] in perfect *W*, respectively. Thus, H and He can migrate quickly until they are tightly trapped by a vacancy, forming $VacH_n$ and $VacHe_n$ clusters, respectively. The binding energy of $VacH_n$ cluster decreases with the increase of the H atom number. The calculated binding energies show that one vacancy is able to trap up to 12 H atoms. The additional H atoms are repulsive to $VacH_{12}$ clusters. The ground-state configurations for $VacH_n$ clusters obtained here are very similar to the results by Ohsawa *et al* [33]. He atoms in the $VacHe_n$ clusters are more energetically favorable to segregation at the center of the vacancy. The systems containing $VacHe_n$ clusters expand and distort more and more strongly when He atoms are increased. With the continuous increase of He atoms, the 15th and 16th He atoms indeed move out of the vacancy. Thus, one vacancy can trap 14 He atoms at most and the additional He atoms prefer to cluster around the $VacHe_{14}$ cluster. The binding energy of $VacHe_n$ clusters shows that He atoms are more strongly trapped in a monovacancy compared with H atoms, and the binding energy decreases from ∼4.6 eV to ∼3 eV and then fluctuates around 2.7 eV even if the He atom number *n* reaches 16.

The presence of $VacH_n$ and $VacHe_n$ clusters in tungsten inevitably induces local distortion and stress. As shown in

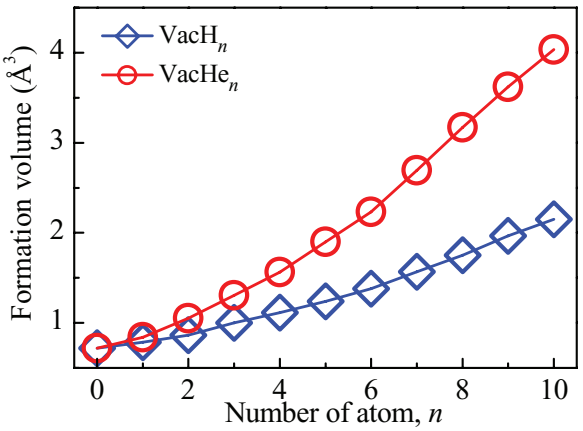

Figure 1. The formation volumes of the systems containing VacH$_n$ and VacHe$_n$ clusters.

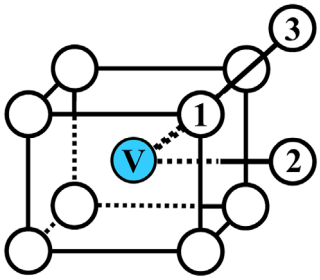

Figure 2. The schematic structure of 1NN, 2NN and 3NN tungsten atoms nearby a VacH$_n$ or VacHe$_n$ cluster. The balls labeled '1', '2' and '3' represent 1NN, 2NN and 3NN tungsten atoms, respectively, and the unlabeled balls are other 1NN tungsten atoms. The ball labeled 'V' represents a VacH$_n$ or VacHe$_n$ cluster.

figure 1, the formation volume of the system containing a VacH$_n$ cluster increases exponentially with the number of H atoms in the cluster. When H atoms add up to 12, the formation volume reaches 2.5 Å^3. In contrast, the formation volume of the system containing a VacHe$_n$ cluster is always larger than that of VacH$_n$. The formation volume difference of the two systems containing VacHe$_n$ and VacH$_n$ clusters increases with n. The increased formation volume indicates significant expansion and increased stress around VacHe$_n$ and VacH$_n$ clusters which, in turn, affects the stability of the tungsten atoms around the two kinds of clusters.

In order to access the stability of tungsten atoms around VacH$_n$ and VacHe$_n$ clusters, we systematically calculate the vacancy-formation energies around the two clusters using equation (4). The first-nearest-neighbor (1NN), second-nearest-neighbor (2NN) and third-nearest-neighbor (3NN) tungsten atoms around a VacH$_n$ or VacHe$_n$ cluster are schematically shown in figure 2. The 1NN, 2NN and 3NN vacancy-formation energies around a pre-existing vacancy are 3.16 eV, 3.52 eV and 3.22 eV, respectively. The 1NN, 2NN and 3NN vacancy-formation energies around the VacH$_n$ and VacHe$_n$ clusters as a function of the number of H or He atom n are displayed in figure 3. Initially, the 1NN, 2NN and 3NN vacancy-formation energies of the VacH$_n$ cluster are very close to that of the pre-existing vacancy. This is because the number of H atoms in the clusters is very small, and it is not sufficient to influence the vacancy-formation energies close to the VacH$_n$

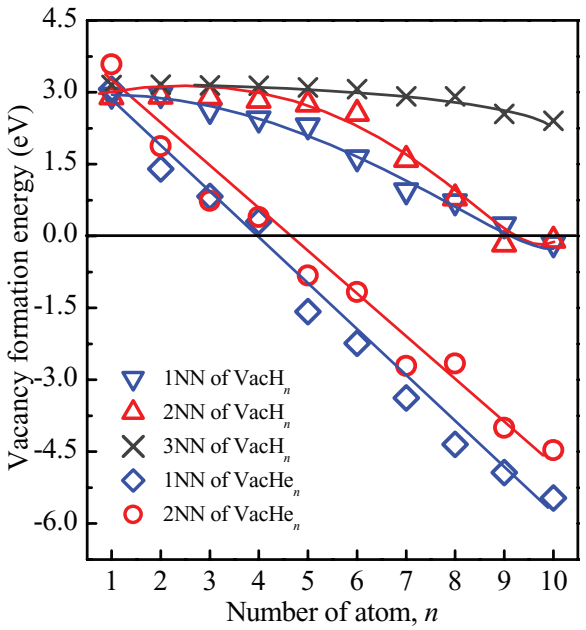

Figure 3. The 1NN, 2NN and 3NN vacancy-formation energies close to VacH$_n$ and VacHe$_n$ clusters as a function of the trapped H or He atoms. Lines are guides to the eyes.

cluster. When the number of H atoms is increased from 1 to 5, the 1NN and 2NN vacancy-formation energies of the VacH$_n$ cluster are slowly reduced in a step-like way. When H atoms add up to 10, the 1NN and 2NN vacancy-formation energies are significantly decreased to 0. Compared to the remarkable reduction of the 1NN and 2NN vacancy-formation energies, the 3NN vacancy-formation energy decreases very weakly. The 3NN vacancy-formation energy is only reduced by 0.5 eV even if the number of H atoms reaches 10. Moreover, the 1NN vacancy-formation energy is relatively small compared to the 2NN vacancy-formation energy. In the case of a VacHe$_n$ cluster, the 3NN vacancy-formation energies close to a VacHe$_n$ cluster are not included due to the computational cost. The 1NN and 2NN vacancy-formation energies of the VacHe$_1$ cluster are nearly not reduced. Then, the 1NN and 2NN vacancy-formation energies close to the VacHe$_n$ cluster decrease sharply (and almost linearly) until He atoms trapped inside the vacancy add up to 10. It is found that both 1NN and 2NN vacancy-formation energies are lower than 0 when the He atom number is more than 4. As the He atoms in the VacHe$_n$ cluster increase, the 1NN and 2NN vacancy-formation energies are further decreased. The 1NN vacancy-formation energies close to the VacHe$_{10}$ cluster are −5.46 eV, which may result in the emission of tungsten atoms from the vicinity of the VacHe$_n$ cluster when n is more than 9 [22]. The stability of 1NN and 2NN tungsten atoms close to the VacHe$_n$ cluster are more substantially reduced compared with those close to VacH$_n$.

The clustering of vacancies in the presence of H and He atoms in tungsten is calculated using equation (5), and the results are presented in figure 4. Up to three vacancies and six H and He atoms are considered. A 128-atom supercell may be not large enough to avoid the interaction of clusters with its mirror image in the periodic supercell. Then, a 250-atom

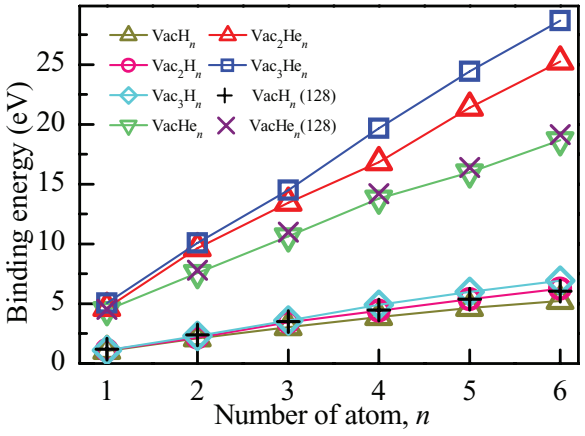

Figure 4. The binding energies of two vacancies and three vacancy clusters in the presence of H and He atoms. The binding energies of VacH$_n$ and VacHe$_n$ clusters are compared in 128-atom and 250-atom supercells.

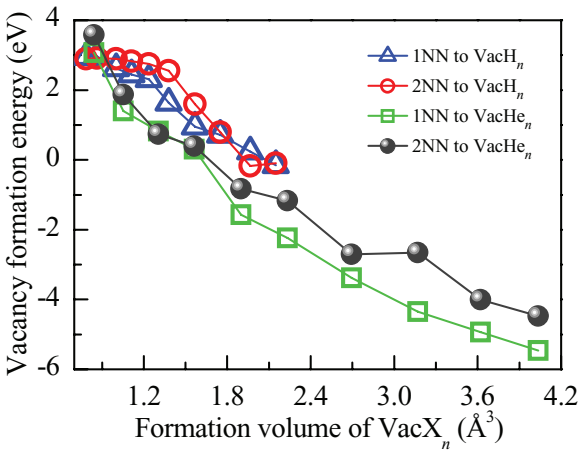

Figure 5. The vacancy-formation energies close to the VacH$_n$ and VacHe$_n$ clusters as a function of formation volumes of the clusters.

supercell is used to calculate the binding energies of H and He with one vacancy, and we find that the binding energies of VacH$_n$ and VacHe$_n$ clusters in a 250-atom system agree well with those in a 128-atom system. Thus, the calculations in a 250-atom system are performed to access the clustering of vacancies in the presence of H and He atoms. Most of previous available empirical and semi-empirical potential calculations predicted that two vacancies attract each other in different configurations [34–39], except the results obtained by Mundim *et al* [40]. Our *ab initio* calculations in 128-atom and 250-atom supercells show that two vacancies repel each other, which agrees well with the results by Becquart *et al* and Oda *et al* [41, 42]. Our calculations show that the binding energies of three vacancies in a 250-atom supercell also show a repulsive interaction and the binding energy is ~ -0.34 eV. In contrast, the interactions of two and three vacancies become attractive in the presence of H and He. The binding energy of Vac$_2$H calculated here is 2.09 eV, which agrees with the value of 1.8 eV obtained by Kato *et al* [43]. The slight difference originates from the relatively large supercell used here. The binding energies of Vac$_2$H$_n$ and Vac$_3$H$_n$ clusters increase with the increase of the H atom number in the vacancy clusters, and reach 6.42 eV and 7.24 eV, respectively. The effect of He in promoting the binding of vacancies is much more significant, and the binding energies of Vac$_2$He$_6$ and Vac$_3$He$_6$ clusters reach 23.86 eV and 27.46 eV, respectively. Thus, the presence of H and He atoms can promote the clustering of vacancies in tungsten remarkably.

3.3. The factors controlling the stability of tungsten atoms around VacH$_n$ and VacHe$_n$ clusters

As discussed in section 3.2, the presence of VacH$_n$ and VacHe$_n$ clusters in tungsten inevitably induces local expansion and stress, which can induce new vacancy formation around the clusters. The concrete relationship between the formation volumes of VacH$_n$ and VacHe$_n$ clusters and the vacancy-formation energies close to the clusters is shown in figure 5. Generally, the 1NN and 2NN vacancy-formation energies close to both VacH$_n$ and VacHe$_n$ clusters decrease as the cluster formation volume increases. The increase of formation volume indicates an increase of stress around the clusters. The presence of a vacancy close to the clusters can release the stress. The greater stress produced around the VacH$_n$ and VacHe$_n$ clusters will be released by a new vacancy. Thus, the interactions of a vacancy with VacH$_n$ and VacHe$_n$ clusters are attractive.

On the other hand, the increase of the formation volume of VacH$_n$ and VacHe$_n$ induces the changes of bond length around the clusters. As shown in figure 6(*a*), both the averaged bond lengths of the 1NN and 2NN *W*–*W* bonds around VacH$_n$ clusters increase when n is increased from 1 to 10. The bond length of the 1NN *W*–*W* bond is increased by 0.03 Å, and similarly the length is increased for the 2NN *W*–*W* bond. The bond lengths of the 1NN and 2NN *W*–*W* bonds around VacHe$_n$ clusters also increase with the number of He atoms. The *W*–*W* bond lengths close to VacHe$_n$ are more significantly increased (figure 6(*b*)). The increased *W*–*W* bond length weakens the *W*–*W* interactions, causing the reduction of the 1NN and 2NN vacancy-formation energies.

The weakened *W*–*W* interactions can also be reflected in the electron density depletion across 1NN, 2NN and 3NN tungsten atoms around VacH$_n$ and VacHe$_n$ clusters. Here, VacH$_6$ and VacHe$_6$ clusters are taken as examples. The electron densities of (1 1 0) planes across 1NN, 2NN and 3NN tungsten atoms around the vacancy, VacH$_{10}$ and VacHe$_6$ are shown in figures 7(*a*)–(*c*), respectively. The 1NN, 2NN, and 3NN tungsten atoms are denoted by A$_n$, B$_n$ and C$_n$ ($n = 1,2$). The charge map is continuous between 1NN, 2NN, and 3NN tungsten atoms for the situation of a vacancy. However, figure 7(*b*) shows that the segregation of 10 H atoms in the single vacancy directly results in the disappearance of the dark gray region between A$_1$ and B$_1$ *W* atoms, and between A$_2$ and B$_2$ *W* atoms. Meanwhile, the dark gray region between A$_1$ and B$_2$ *W* atoms also shrinks. However, the dark gray region between A$_1$ and C$_1$ (C$_2$) is nearly unaffected compared with that in figure 7(*a*). The dark gray regions between A$_1$ (A$_2$) and B$_1$ (B$_2$) are more significantly reduced in figure 7(*c*), while the dark gray regions between A$_1$ and C$_1$ (C$_2$) are slightly affected. The reduction of dark region indicates the depletion

of electron density, which weakens the bonding of *W* with its closest *W* atom. All these factors contribute to the instability of the 1NN and 2NN tungsten atoms around the $VacH_n$ and $VacHe_n$ clusters.

Moreover, the charge analysis is conducted around the $VacH_n$ and $VacHe_n$ clusters. Bader's theory of atoms is often useful for charge analysis [44]. The charge enclosed within the Bader volume is a good approximation to the total electronic charge of an atom. The averaged charge on the H and He atoms in the $VacH_n$ and $VacHe_n$ clusters, and the charge on the 1NN, 2NN and 3NN tungsten atoms around the clusters are shown in figure 8. The positive value suggests charge gain while a negative result means charge depletion. The Bader's charge analysis (figure 8(*a*)) shows the charge on the 1NN and 2NN tungsten atoms around the $VacH_n$ cluster has moved away. As the H atoms in the $VacH_n$ cluster increase, the charge is further transferred, and the charge on the 1NN and 2NN tungsten atoms is −0.45 e and −0.26 e when *n* reaches 10. In contrast, the charge on the 3NN tungsten atoms is almost unaffected. As shown in figure 8(*b*), the averaged charge gain on the H atoms in the $VacH_n$ cluster keeps at about 0.6 e. So the charge on the surrounding tungsten atoms move to the $VacH_n$ cluster. This may be the reason why the *W*–*W* bond is weakened, and the H atoms in the cluster repel each other due to the Coulomb interactions. As for the $VacHe_n$ cluster, the charge on the 1NN, 2NN and 3NN tungsten atoms around the $VacHe_n$ cluster is slightly affected, and the averaged charge on the He atoms is only 0.12 e (see figures 8(*c*) and (*d*)). Therefore, the instability of the tungsten atoms around the $VacHe_n$ cluster may not originate from the charge reduction on each tungsten atom. The significantly increased *W*–*W* bond length weakens the *W*–*W* bond and the local stress may be the main reason for the instability of the tungsten atoms around the $VacHe_n$ clusters.

3.4. The diffusion of $VacH_n$ and $VacHe_n$ clusters

The mobilities of H, He, vacancies, and H and He-containing vacancy clusters have a big influence on the microstructural evolution of tungsten in a fusion environment. The diffusion of H and He in perfect tungsten and through a vacancy has been widely studied in previous works [32, 45–47]. It is found H and He can diffuse with barriers as low as ∼0.20 eV [47] and 0.06 eV [32] in tungsten, respectively. The presence of a vacancy usually impedes the diffusion of H and He in tungsten. The escaping barriers of H (∼1.39 eV) and He (∼4.61 eV) from a vacancy approximate the binding energies of H and He with a vacancy plus the barriers of H and He in perfect tungsten, respectively. However, a monovacancy can move with a barrier of 1.78 eV along the (1 1 1) direction in tungsten [42]. In the presence of H and He, the mobility of the vacancy becomes complicated. Here, we take the diffusion of a VacH cluster as an example, and the obtained results are shown in figure 9. For the VacH cluster, the H atom occupies an octahedral site close to the vacancy center, i.e. the first structure in the inset of figure 9. When the VacH cluster migrates along the (1 1 1) direction, the vacancy diffuses to the first-nearest-neighbor lattice site and the H atom moves to the

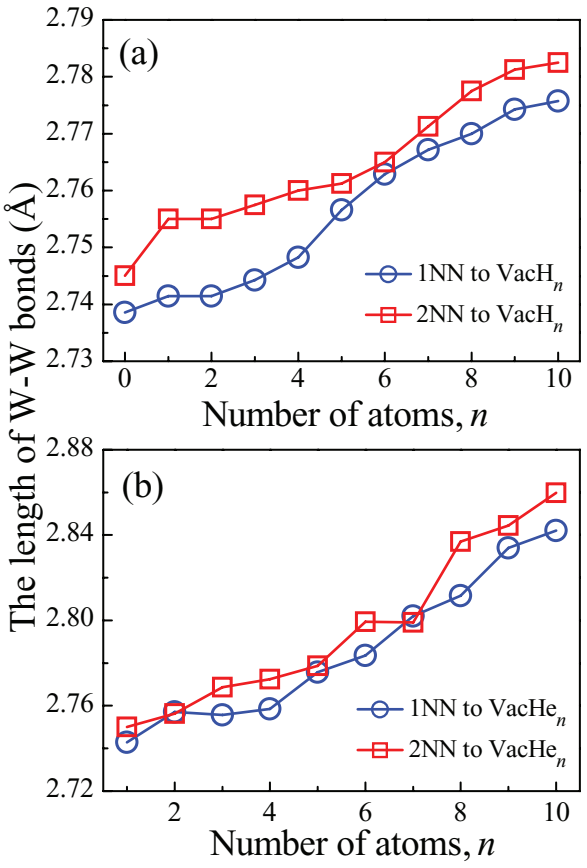

Figure 6. The averaged tungsten–tungsten bond length in the 1NN and 2NN around the $VacH_n$ (*a*) and $VacHe_n$ (*b*) clusters as a function of the trapped H and He atoms, respectively.

octahedral site close to the new site of the vacancy, and the diffusion barrier of the VacH cluster reaches up to 2.56 eV. Only H is associated with the following diffusion, and the H atom moves away from the vacancy to the tetrahedral interstitial site with an energy barrier of 0.89 eV. Then, H continually diffuses away from the vacancy, and the barrier gradually decreases to 0.35 eV and then approaches that of H in perfect tungsten. These diffusion paths constitute all the migration processes of a VacH cluster. Generally, the presence of H somewhat slows down the migration of the vacancy in tungsten. As for a VacHe cluster, the situation will be more complicated as He atoms prefer the vacancy center. The VacHe cluster may move due to the way that He atom firstly jumps out to the interstitial site, and the vacancy moves to the closest lattice site, and finally the He atom diffuses to the vacancy in the new site at last. We tried this way, however, and no saddle point was found. Thus, the diffusion of the $VacHe_n$ cluster needs to be systemically investigated.

4. Discussion

During the lifetime, the PFMs will be subject to high-flux, low-energy, and steady-state hydrogen isotopes and helium plasma bombardment. Additionally, H and He atoms are also transmuted due to high-energy neutron irradiation. The interplay of H and He atoms with an irradiation-induced defect-like

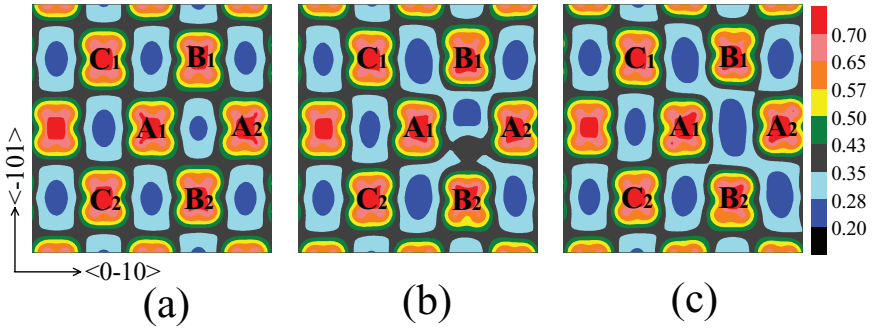

Figure 7. The electron density maps (electron/Å^3) of three different cases: the empty vacancy (*a*), the $VacH_{10}$ (*b*) and $VacHe_6$ (*c*) clusters. In all cases, the slices are cut through the same (1 1 0) plane of the supercell considered. A_n, B_n, C_n denote the 1NN, 2NN and 3NN *W* atoms of the vacancy, $VacH_{10}$ and $VacHe_6$ clusters. The subscripts 1 and 2 are used to distinguish different atoms.

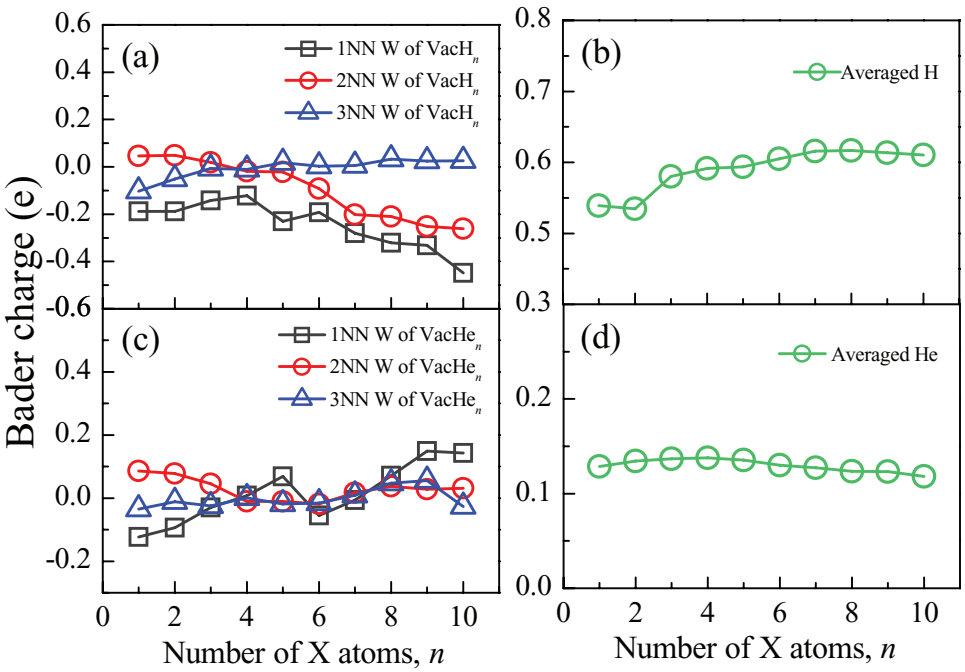

Figure 8. The Bader charge of 1NN, 2NN and 3NN tungsten atoms close to $VacH_n$ (*a*), $VacHe_n$ (*c*) clusters. The averaged bader charge on H (*b*) and He (*d*) atoms in $VacH_n$ and $VacHe_n$ clusters, respectively.

vacancy has big influence on the microstructure evolution of tungsten, for example, leading to H and He bubble formation. Bubbles are unfavorable since they cause the degradation of tungsten. Many experiments have been performed to investigate the phenomena of H and He bubble formation. However, the underlying atomic mechanism controlling the formation of bubbles from the behaviors of H and He atoms is still difficult to access directly by experiment. Simulation is a good supplement to the experimental study of H and He bubbles at the atomic scale. By performing *ab initio* and molecular dynamics simulations, it has been widely recognized that a vacancy can act as a trapping center for both H and He atoms in tungsten [6–9, 22, 32, 48]. It has been found that a monovacancy is able to accommodate up to 12 H atoms and 14 He atoms. The present binding energies and configurations of vacancy–hydrogen and vacancy–helium clusters obtained agree well with the *ab initio* results by Ohsawa *et al* [8], Heinola *et al* [9], and Becquart *et al* [41]. Our results regarding the vacancy–hydrogen binding energies also agree with the values estimated from experimental measurements with an ^{111}In probe [49]. The formation of vacancy–hydrogen and vacancy–helium clusters could act as a nucleation point of H and He bubbles. However, the gap between vacancy–hydrogen (helium) clusters and bubbles is still not bridged.

The accumulation of multiple H and He atoms at interstitial sites and vacancies induces local expansion of the lattice. The formation volumes of $VacH_{10}$ and $VacHe_{10}$ clusters reach 2.5 Å^3 and 4.04 Å^3, respectively. The stress induced by the clusters may cause the mutation of $VacH_n$ and $VacHe_n$, and the clusters grow until the formation of bubbles occurs. Many experiments have tried to understand the underlying atomic mechanism for the mutation of $VacH_n$ and $VacHe_n$ clusters in tungsten. Abd El Keriem *et al* found that the growth of a vacancy happens when the vacancy is filled to an occupation of about 10 He atoms with the ^{111}In probe [23]. Our calculated results agree very well with the experimental results [23]. In our previous simulation work [22], the emission of surrounding tungsten atoms

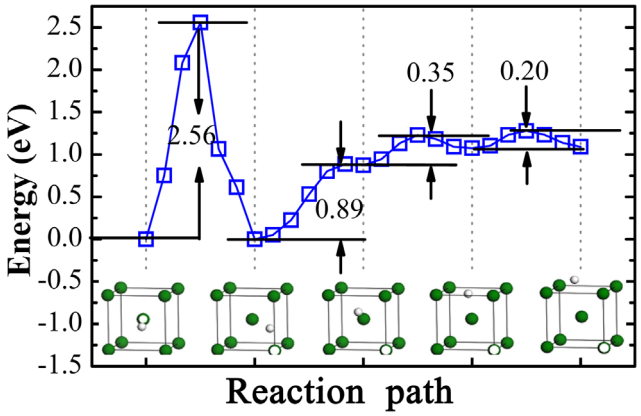

Figure 9. The diffusion barrier profile and paths of a VacH cluster in tungsten. The inset is the detailed configuration of H relative to the vacancy.

of Vac_0He_n (He_n) and Vac_1He_n ($VacHe_n$) clusters is also found to be possible once n is beyond 5 and 9, respectively. However, we find that emission of tungsten atoms from Vac_mH_n clusters is relatively difficult. How the stress effect around $VacH_n$ and $VacHe_n$ clusters works on the mutation of the clusters still needs to be ascertained. This is because H and He clusters situated at interstitial sites and vacancies induce local distortion and stress, and the appearance of a vacancy can release the stress, and make the system more stable. Therefore, the vacancy-formation energies close to Vac_mH_n and Vac_mHe_n clusters are calculated. According to our results, above, the 1NN and 2NN vacancies close to both $VacH_n$ and $VacHe_n$ clusters are significantly reduced. The vacancy-formation energies close to Vac_mHe_n clusters are much more significantly reduced compared with those close to Vac_mH_n clusters. Thus, the stability of the tungsten atoms around the Vac_mHe_n clusters is more substantially reduced. This may be the reason why the emission of tungsten atoms from the vicinity of Vac_mHe_n clusters is possible, while the emission of tungsten atoms from Vac_mH_n clusters is difficult [22]. We also calculate the vacancy-formation energies close to $VacHe_n$ clusters at the (1 0 0) surface to understand the effect of the surface on the emission of tungsten atoms. Here, only the situation of the (1 0 0) surface and 6 He atoms is considered to avoid too much computation cost. We used $p(4 \times 4)$ surface and a k-point sampling of $1 \times 1 \times 1$. Nineteen layers were used and the last four layers were fixed. We used a 20 Å -thick vacuum layer. The results obtained show that the vacancy-formation energy closest to $VacHe_6$ is -14.60 eV in the third layer of the surface. The stability of tungsten atoms close to $VacHe_n$ in the surface is more markedly reduced compared with that in bulk. Similar results are found in the sixth and eighth layers. These results indicate that the mutation of $VacHe_n$ is relatively easy near the surface. Thus, the interface also plays an important role in the microstructure evolution of tungsten, as discussed by Hu *et al* [50, 51]. When a new vacancy is produced close to Vac_mHe_n clusters, the vacancy will be tightly captured by the cluster since the presence of He could significantly promote the clustering of vacancies.

The decrease in stability just suggests that the emission of tungsten atoms becomes easy. It does not denote that the emission of tungsten atoms becomes spontaneous. Although the emission of tungsten atoms from the vicinity of Vac_mH_n clusters is relatively difficult without any perturbation, the stability of tungsten atoms around the clusters is definitely decreased. In an experimental environment, the knock-on of other H (He) ions or perturbation may facilitate the emission of tungsten atoms from the vicinity of Vac_mH_n and Vac_mHe_n clusters. This may result in vacancy formation even if no displacement damage appears in tungsten under low-energy H and He ion irradiation. H and He segregate in these vacancies forming $VacH_n$ and $VacHe_n$ clusters which probably become Vac_2H_n and Vac_2He_n clusters, respectively. The further calculations show that the vacancy-formation energies closest to Vac_2H_{10} and Vac_2He_{10} clusters are reduced to 1.87 eV and -2.26 eV, respectively. Similarly, the vacancy-formation energies around the Vac_3H_{10} and Vac_3He_{10} are also significantly reduced. The emission of surrounding tungsten atoms from Vac_mH_n and Vac_mHe_n clusters results in the growth and evolution of vacancy clusters, and the presence of H and He atoms, in turn, promotes the tight binding of the vacancy clusters. Then, the vacancy clusters continuously trap H and He atoms, which results in the ultimate formation of H and He bubbles, respectively. The emission of tungsten atoms from the vicinity of Vac_mH_n and Vac_mHe_n clusters is probably the reasons why H and He bubbles with diameters of a few to hundreds of microns can form on a W surface even if the ion energy is so low that no displacement damage is created [13, 16, 52–55].

Additionally, it is reported that He will form bubbles at $\sim$100 Å to the W surface, while H bubbles are found at micrometer depths [52–57]. The results can also be qualitatively explained by the present results. According to our calculations, the formation of interstitial H clusters are energetically unfavorable. H is favorable to segregation in a vacancy; however, the interaction between interstitial H atom with $VacH_{12}$ clusters is also repulsive. In contrast, interaction of interstitial He atoms pairs are energetically preferable, and He atoms even form close-packed monolayer He interstitial clusters [22]. Meanwhile, there exists strongly attractive interaction of interstitial He atoms with vacancies and $VacHe_{14}$ clusters. Thus, low-energy He atoms can be easily attracted to the $VacHe_n$ cluster or the other interstitial He atoms, which thereby impedes the migration of He atoms deeper into the tungsten bulk. In contrast, when low-energy H atoms diffuse into tungsten, H atoms may be bound by a vacancy or vacancy clusters. When the vacancy or vacancy clusters are filled, H atoms cannot bind to other interstitial H atoms, but diffuse deeper into the bulk.

5. Conclusions

Based on first-principles calculations, we have systemically investigated the stability of tungsten atoms around both hydrogen and helium clusters at interstitial sites and vacancies. We find that the vacancy-formation energies closest to

interstitial hydrogen and helium clusters are significantly reduced, and the first-nearest and second-nearest-neighbor vacancy-formation energies close to vacancy–hydrogen and vacancy–helium clusters are remarkably decreased. The vacancy-formation energies close to helium clusters are significantly more reduced than those of nearby hydrogen clusters notwithstanding that the clusters are embedded at interstitial sites or vacancies. The reduced vacancy-formation energy suggests stability of tungsten atoms nearby clusters is more markedly lowered. These findings illustrate the experimental results which explain why the emission of tungsten atoms from the vicinity of vacancy–helium clusters is possible. The emission of tungsten atoms from hydrogen clusters is also possible once environment perturbation occurs. The emission of surrounding tungsten atoms from hydrogen and helium clusters results in the growth of vacancy clusters and H and He atoms, in turn, promote the tight binding of the vacancy clusters. The vacancy clusters continuously trap H and He atoms, resulting in the ultimate formation of bubbles. These results explain the bubble formation even if no displacement is produced in tungsten exposed to low-energy hydrogen and helium ion irradiation. In addition, our results illustrate the different deposition depth of hydrogen and helium in tungsten even when the migration rate of helium is far larger than that of hydrogen.

Acknowledgments

This work was supported by the National Magnetic Confinement Fusion Program (Grant No 2015GB112001), the National Natural Science Foundation of China (Nos 11405202, 11505229 and 11375231), the Youth Innovation Promotion Association of CAS (2015384) and the Center for Computation Science, Hefei Institutes of Physical Sciences. This research project was part of the CRP (Co-ordinated Research Projects) program carried out under the sponsorship of the International Atomic Energy Agency.

References

[1] ITER Physics Basis Editors *et al* 1999 *Nucl. Fusion* **39** 2137
[2] Gilliam S.B., Gidcumb S.M., Parikh N.R., Forsythe D.G., Patnaik B.K., Hunn J.D., Snead L.L. and Lamaze G.P. 2005 *J. Nucl. Mater.* **347** 289
[3] Gilliam S.B., Gidcumb S.M., Forsythe D.G., Parikh N.R., Hunn J.D., Snead L.L. and Lamaze G.P. 2005 *Nucl. Instrum. Methods Phys. Res.* B **241** 491
[4] Ueda Y., Funabiki T., Shimada T., Fukumota K., Kurishita H. and Nishikawa M. 2005 *J. Nucl. Mater.* **337–9** 1010
[5] Xu Q., Yoshida N. and Yoshiie T. 2007 *J. Nucl. Mater.* **367–70** 806
[6] Liu Y.L., Zhang Y., Zhou H.B., Lu G.H., Liu F. and Luo G.N. 2009 *Phys. Rev.* B **79** 172103
[7] Jiang B., Wan F.R. and Geng W.T. 2010 *Phys. Rev.* B **81** 134112
[8] Ohsawa K., Goto J., Yamakami M., Yamaguchi M. and Yagi M. 2010 *Phys. Rev.* B **82** 184117
[9] Heinola K., Ahlgren T., Nordlund K. and Keinonen J. 2010 *Phys. Rev.* B **82** 094102
[10] Fukai Y. and Ōkuma N. 1994 *Phys. Rev. Lett.* **73** 1640
[11] Fukai Y. 1995 *J. Alloys Compd.* **231** 35
[12] Fukai Y. 2003 *Phys. Scr.* **T103** 11
[13] Miyamoto M., Nishijima D., Ueda Y., Doerner R.P., Kurishita H., Baldwin M.J., Morito S., Ono K. and Hanna J. 2009 *Nucl. Fusion* **49** 065035
[14] Lindig S., Balden M., Alimov V.K., Yamanishi T., Shu W.M. and Roth J. 2009 *Phys. Scr.* **T138** 014040
[15] Shu W.M., Wakai E. and Yamanishi T. 2007 *Nucl. Fusion* **47** 201
[16] Shu W.M., Kawasuso A., Miwa Y., Wakai E., Luo G.N. and Yamanishi T. 2007 *Phys. Scr. T* **128** 96
[17] Shu W.M. 2008 *Appl. Phys. Lett.* **92** 211904
[18] Ogorodnikova O.V., Roth J. and Mayer M. 2008 *J. Appl. Phys.* **103** 034902
[19] Nishijima D., Ye M.Y., Ohno N. and Takamura S. 2004 *J. Nucl. Mater.* **329–33** 1029
[20] Henriksson K.O.E., Nordlund K., Keinonen J., Sundholm D. and Patzschke M. 2004 *Phys. Scr. T* **108** 95
[21] Henriksson K.O.E., Nordlund K. and Keinonen J. 2006 *Nucl. Instrum. Methods Phys. Res.* B **244** 377
[22] You Y.W., Li D.D., Kong X.S., Wu X.B., Liu C.S., Fang Q.F., Pan B.C., Chen J.L. and Luo G.N. 2014 *Nucl. Fusion* **54** 103007
[23] El Keriem M.S.A., van der Werf D.P. and Pleiter F. 1993 *Phys. Rev.* B **47** 14771
[24] Kresse G. and Furthmüller J. 1996 *Phys. Rev.* B **54** 11169
[25] Kresse G. and Hafner J. 1993 *Phys. Rev.* B **47** 558
[26] Perdew J.P., Chevary J.A., Vosko S.H., Jackson K.A., Pederson M.R., Singh D.J. and Fiolhais C. 1992 *Phys. Rev.* B **46** 6671
[27] Monkhorst H.J. and Pack J.D. 1976 *Phys. Rev.* B **13** 5188
[28] Lee S.C., Choi J.H. and Lee J.G. 2009 *J. Nucl. Mater.* **383** 244
[29] Becquart C.S. and Domain C. 2009 *J. Nucl. Mater.* **386–8** 109
[30] Liu Y.L., Zhang Y., Luo G.N. and Lu G.H. 2009 *J. Nucl. Mater.* **390–1** 1032
[31] Becquart C.S. and Domain C. 2006 *Phys. Rev. Lett.* **97** 196402
[32] Zhou H.B., Liu Y.L., Jin S., Zhang Y., Luo G.N. and Lu G.H. 2010 *Nucl. Fusion* **50** 115010
[33] Ohsawa K., Eguchi K., Watanabe H., Yamaguchi M. and Yagi M. 2012 *Phys. Rev.* B **85** 094102
[34] Johnson R.A. and Wilson W.D. 1972 *Interatomic Potentials and Simulation of Lattice Defects* eds Gehlen P.C. (New York: Plenum) p 301
[35] Wilson W.D. and Bisson C.L. 1974 *Radiat. Eff.* **22** 63
[36] Masuda K. 1982 *J. Phys.* **43** 921
[37] Johnson R.A. 1983 *Phys. Rev* B **27** 2014
[38] van Veen A. 1987 *Mater. Sci. Forum* **15–8** 3
[39] Hu W., Shu W. and Zhang B. 2002 *Comput. Mater. Sci.* **23** 175
[40] Mundim K.C., Malbouisson L.A., Dorfman S., Fuks D., Van Humbeek J. and Liubich V. 2001 *J. Mol. Struct.* **539** 191
[41] Becquart C.S. and Domain C. 2007 *Nucl. Instrum. Methods Phys. Res.* B **255** 23
[42] Oda Y., Ito A.M., Takayama A. and Nakamura H. 2014 *Plasma Fusion Res.* **9** 3401117
[43] Kato D., Iwakiri H. and Morishita K. 2011 *J. Nucl. Mater.* **417** 1115
[44] Bader R.W.F. 1990 *Atoms in Molecules: A Quantum Theory* (Oxford: Oxford University Press)
[45] You Y.W., Kong X.S., Wu X.B., Xu Y.C., Fang Q.F., Chen J.L., Luo G.N., Liu C.S., Pan B.C. and Wang Z.G. 2013 *AIP Adv.* **3** 012118
[46] Kong X.S., Wang S., Wu X.B., You Y.W., Liu C.S., Fang Q.F., Chen J.L. and Luo G.N. 2015 *Acta Mater.* **84** 426
[47] Heinola K. and Ahlgren T. 2010 *J. Appl. Phys.* **107** 113531
[48] Kato D., Iwakiri H. and Morishita K. 2009 *J. Plasma Fusion Res. Ser.* **8** 404
[49] Fransens J.R., El Keriem M.S.A. and Pleiter F. 1991 *J. Phys.: Condens. Matter* **3** 9871

[50] Hu L., Hammond K.D., Wirth B.D. and Maroudas D. 2014 *Surf. Sci.* **626** L21
[51] Hu L., Hammond K.D., Wirth B.D. and Maroudas D. 2014 *J. Appl. Phys.* **115** 173512
[52] Sze F.C., Doerner R.P. and Luckhardt S. 1999 *J. Nucl. Mater.* **264** 89
[53] Haasz A.A., Poon M. and Davis J.W. 1999 *J. Nucl. Mater.* **266–9** 520
[54] Sze F.C., Chousal L., Doerner R.P. and Luckhardt S. 1999 *J. Nucl. Mater.* **266–9** 1212
[55] Iwakiri H., Yasunaga K., Morishita K. and Yoshida N. 2000 *J. Nucl. Mater.* **283–7** 1134
[56] Alimov V.K., Roth J. and Mayer M. 2005 *J. Nucl. Mater.* **337–9** 619
[57] Henriksson K.O.E., Nordlund K., Krasheninnikov A. and Keinonen J. 2006 *Fusion Sci. Technol.* **50** 43